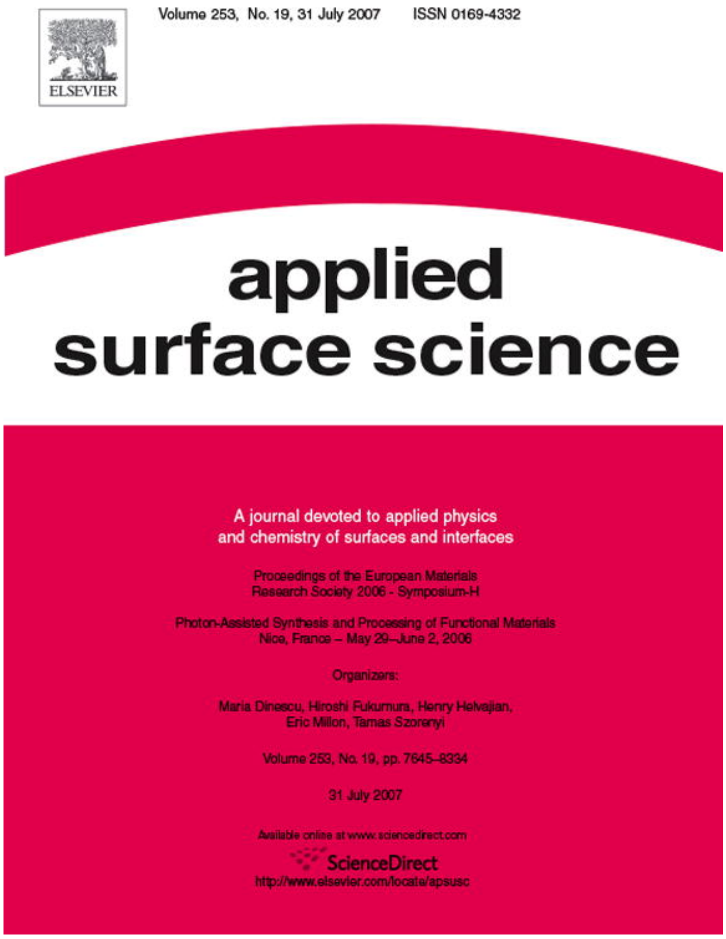
Volume 253, No. 19, 31 July 2007 ISSN 0169-4332
ELSEVIER
applied surface science
A journal devoted to applied physics and chemistry of surfaces and interfaces
Proceedings of the European Materials Research Society 2006 - Symposium-H
Photon-Assisted Synthesis and Processing of Functional Materials
Nice, France – May 29–June 2, 2006
Organizers:
Maria Dinescu, Hiroshi Fukumura, Henry Helvajian, Eric Millon, Tamas Szorenyi
Volume 253, No. 19, pp. 7645–8334
31 July 2007
Available online at www.sciencedirect.com
ScienceDirect
http://www.elsevier.com/locate/apsusc

Available online at www.sciencedirect.com
ScienceDirect
Applied Surface Science 253 (2007) 7744–7748
applied surface science
www.elsevier.com/locate/apsusc

Transient effects in pulsed laser irradiation

V.I. Mazhukin [a], M.G. Lobok [a], I. Smurov [b,*]

[a] *Institute of Mathematical Modeling of RAS, 4a Miusskaya sqr., 125047 Moscow, Russia*

[b] *Ecole Nationale d'Ingénieurs de Saint-Etienne (ENISE), DIPI Laboratory, 58 rue Jean Parot, 42023 Saint-Etienne Cedex 2, France*

Available online 25 February 2007

Abstract

Theoretical analysis of the influence of the temporal profile (rectangular, triangular, Gaussian) of the laser pulse on heating/cooling and phase transition velocities and quantity of ablated material was performed on the basis of a multifront Stephan problem. Modeling showed that material removal under stationary conditions (that correspond to long pulses) is entirely controlled by specific heat and material density, while in the case of transient regimes (short pulses) thermal conductivity and heat capacity play a predominant role. Interaction of the melting and evaporation fronts characterized by an evaporation front velocity far exceeding the melting front one is one of the examples of the transient nature of the phenomena influenced by the laser pulse parameters.

PACS : 79.20.Ds; 64.70.Dv; 42.62.−b

Keywords: Laser melting; Laser evaporation; Laser pulse shape

1. Introduction

Most of the technological thermal processes of laser treatment of materials are concerned with the first order phase transitions: melting–solidification and evaporation–condensation. The role of the relationship between the depth of the molten pool and the thickness of the evaporated layer is critical in drilling, pulsed cutting and welding. In these processes the size of the molten pool and geometry of the hole depend on both laser irradiation parameters defined by wavelength, pulse duration and time-space distribution of pulse intensity, as well as thermophysical and optical properties of the treated material [1]. To optimize a chosen technological application, the influence of each of these factors must be analyzed and characterized. Fulfilling this task requires modeling of the time-space distribution of temperature fields and the phase transition dynamics. In this purpose a number of mathematical models have been used [2,3].

The published results [4–6] demonstrate a significant role of the transient effects in laser processing. Nevertheless, although a great number of publications consider various issues of laser irradiation, the issue of transient effects is far from being completely studied.

The aim of the present paper is to analyze the transient effects in a wide range of pulse durations and intensities in laser processing of metals with strongly different thermophysical properties such as copper and titanium.

2. Formulation of the problem

Processes of laser heating, melting and evaporation of metals are described in the frame of a joint variant of the Stephan problem including the classical and one-phase approaches [3]. This joint model solves the thermal conductivity equation with boundary conditions at two moving interphases $\Gamma_{sl}(t)$ (solid–liquid) and $\Gamma_{lv}(t)$ (liquid–vapor). Their location is a priori unknown and found in the course of solution through the corresponding boundary conditions. The absorbed laser radiation is assumed to be released in the thin surface layer. The origin of the coordinate frame is situated at the surface of the irradiated target, thereby the melting velocity is directed inwards and thus negative. Consequently, the solidification velocity is positive.

Numerical solution of the system of equations is carried out using a dynamical adaptation [7,8] allowing to explicitly track the phase boundaries.

* Corresponding author. Tel.: +33 4 7791 0161; fax: +33 4 7774 3497.
E-mail address: smurov@enise.fr (I. Smurov).

0169-4332/$ – see front matter
doi:10.1016/j.apsusc.2007.02.086

Two metals with strongly different thermophysical properties were used as target: copper with high thermal conductivity and titanium with low thermal conductivity and high heat of fusion [9,10]. The difference is most pronounced for thermal conductivity which is 10 times higher for copper and for the value of specific heat of vaporization L_v which is 3 times higher for titanium. Absorption of the metallic surface was assumed independent of the temperature and given as $A = 0.1$ that corresponds approximately to the absorption of the polished metals at the $\lambda_l \approx 10.6\ \mu m$ laser radiation.

3. Analysis of the modeling results

Generated by a single laser pulse, a number of sequentially emerging nonlinear processes constitute the dominating mechanism for mass and energy transfer in the irradiation zone. The final result of these competing processes is controlled by a number of laser irradiation parameters. One of them is the energy input rate defined by the temporal profile of the laser pulse. The largest difference in material processing is supposed to be between the cases characterized by a transient energy input (i.e. single pulse) and by those with a steady energy input that, provided a sufficient duration, could establish stationary conditions.

The one-dimensional steady-state evaporation is characterized by the energy balance equation [11]:

$$x = \Gamma_{lv}(t) : G_{sur} = AG$$
$$= \rho_l v_{lv}\left(L_m + L_v + \int_{T_0}^{T_{sur}} C_p(T)\,dT + \sigma T_{sur}^4\right), \qquad (1)$$

The velocity of the evaporation front v_{lv} may be given as the following approximated equality:

$$v_{lv} = \frac{G_{sur}}{\rho_l L_v} \approx v_0 \exp\left(-\frac{L_v}{kT_{sur}}\right) \qquad (2)$$

where v_0 is a velocity close to the sonic velocity in metal, G_{sur} is the absorbed radiation intensity, ρ_l is the density of the liquid state, C_p is the heat capacity, L_v, L_m are the specific heat of vaporization and melting, k is the Boltzmann constant, σ is the Stefan Boltzmann constant.

3.1. Influence of the temporal profile of the laser pulse

Let us analyze heat and mass transfer dynamics between the vapor, liquid and condensed phases for pulses with different temporal profiles but the same energy input and duration.

3.1.1. Rectangular pulse

The rectangular temporal profile, Fig. 1a, $G = \begin{cases} G_0, t \le \tau_l \\ 0, t > \tau_l \end{cases}$, was chosen as reference for the others. The absorbed intensity was $G_{sur} = 10^7$ W cm^{-2}, the pulse duration was $\tau_l = 2 \times 10^{-4}$ s. The values of intensity $G(t)$ and pulse duration τ_l were selected in such a way to make it possible for the system to reach a steady state in terms of both surface temperature T_{sur}, Fig. 2 and phase boundaries velocities $v_{sl}(t)$, $v_{lv}(t)$, Fig. 3.

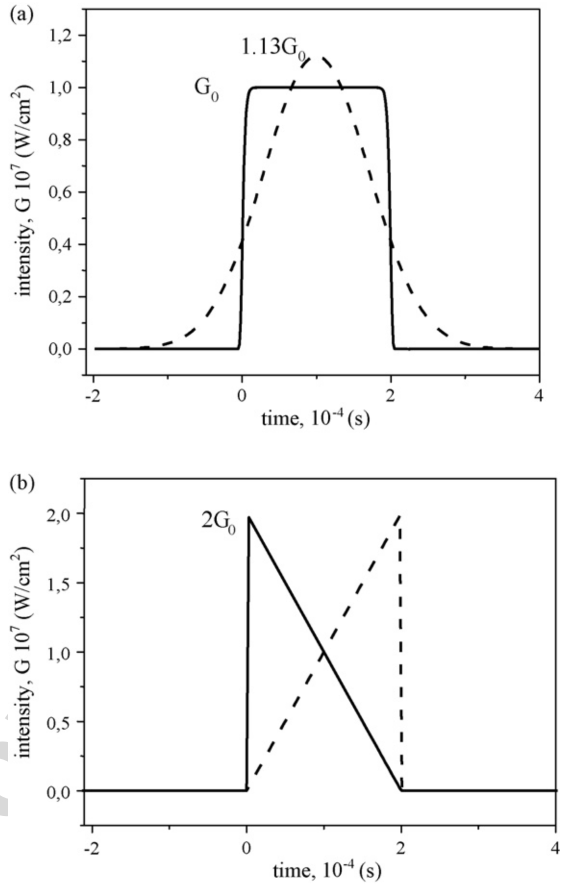

Fig. 1. Pulse temporal profiles: (a) rectangular and Gaussian, (b) right-angled triangular with increasing (rising triangle) and decreasing (falling triangle) energy density fluxes.

A particularity of the rectangular-pulse irradiation is the presence of two transient intervals related to instantaneous changes in intensity, namely the fore and the rear fronts corresponding to the switch-on and the turn-off of the pulse. A jump-like change in intensity at the switch-on of the pulse leads to the formation of a near-surface zone of the maximum temperature gradients. The comparison (Table 1) of the

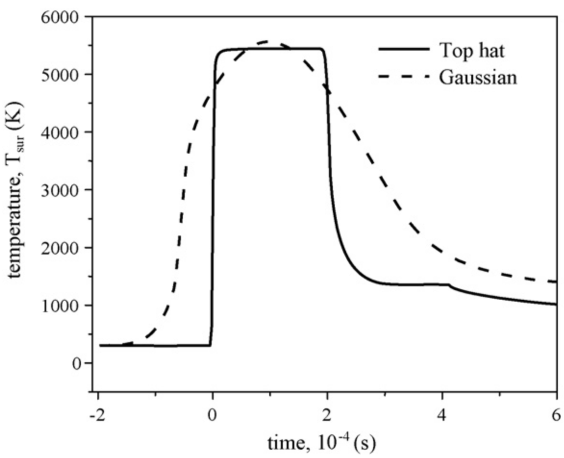

Fig. 2. Evolution of the surface temperature $T_{sur}(t)$ for copper: rectangular (full line) and Gaussian (dashed lime) pulses.

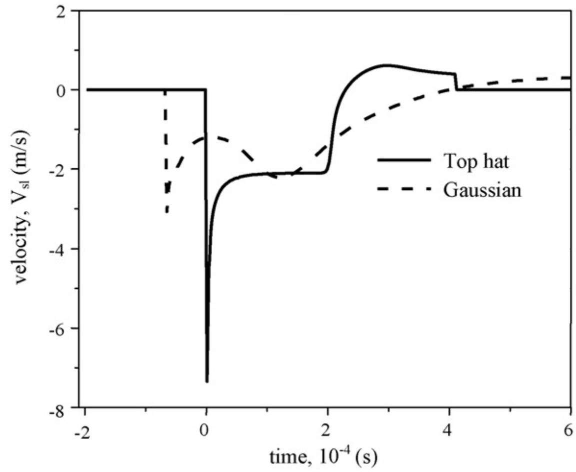

Fig. 3. Evolution of the melting front velocity $v_{sl}(t)$ for copper: rectangular (full line) and Gaussian (dashed line) pulses.

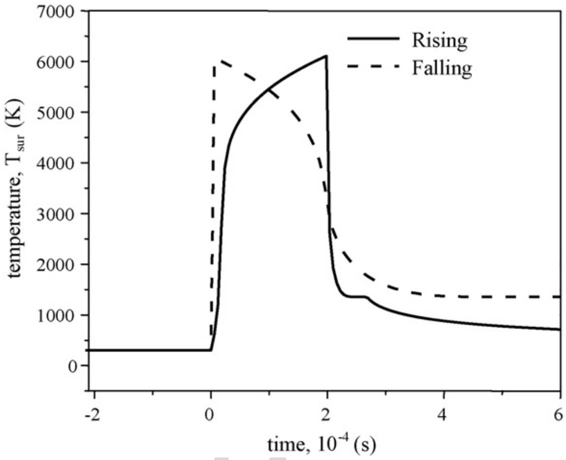

Fig. 4. Evolution of the surface temperature $T_{sur}(t)$ for copper: rising (full line) and falling (dashed lime) triangular pulses.

thickness of the evaporated layer $H_v \cong 410$ μm and of the molten layer $H_v/H_l \cong 5$ for copper and, respectively, $H_v \cong 397$ μm, $H_v/H_l \cong 60$ for titanium demonstrated that the main part of the energy of the rectangular pulse goes to evaporation. The following equations have been used to obtain thickness of the evaporated layer $H_v = \int_{t_0}^{t} v_{lv}\,dt$ and depth of the molten pool $H_l = \int_{t_m}^{t} (v_{sl} - v_{lv})\,dt$, where t_m is the instant when melting starts.

3.1.2. Triangular pulse

Two kinds of right-angled triangles were considered: with increasing (rising triangle) and decreasing (falling triangle) energy density fluxes, Fig. 1b. The processes related to the fronts moving develop qualitatively in the same way that when using the rectangular pulse.

In the right-angled falling triangle the maximum intensity is reached at the switch-on moment. Accordingly, the system demonstrates the highest degree of transience at the beginning of the pulse. In the right-angled rising triangle the maximum intensity and the highest degree of transience are reached at the turn-off moment. For both materials, a two-time increase of the maximum intensity leads to significant, as compared to the rectangular pulse case, quantitative differences at the moment of the fronts moving. These differences are most pronounced for the surface temperature $T_{sur,max}$, Fig. 4 and the evaporation front velocity $v_{lv,max}$, Table 1.

In the case of the falling triangle, transience of the processes is favorable for a smooth change from the surface evaporation to the surface melting as the dominating mechanism. It means that with time more energy of the pulse goes to melting, Fig. 5. In the case of the rising triangle, because of the energy losses related to the target heating at the beginning and the evaporation at the end of the pulse, the melting process in general happens to be less efficient, Fig. 5.

Thus, the major differences for the above considered triangular pulses were observed for the depth of penetration $H_{lv} = H_l + H_v$ and the life-time of the molten pool τ_{lx}, Table 1.

3.1.3. Gaussian profile

The Gaussian pulse, Fig. 1a is the only one among the pulses without sharp fronts and having smooth wings. Such an energy distribution results in the predominant role of the processes of heating and melting of the solid phase. As in the case of the rising triangle, the initiation and the interaction of the phase fronts are widely separated in time. The melting front is initiated at the leading edge of the pulse and, as it may be seen

Table 1
Quantitative comparative analysis of thermal phenomena for copper and titanium under pulsed laser irradiation with different temporal profiles

Pulse temporal profile	Maximum surface temperature (°K)	Maximum evaporation velocity (m/s)	Maximum depth of penetration (m)	Maximum thickness of evaporated layer (m)	Maximum depth of the molten pool (m)	Melt life-time (s)
Copper						
Rectangle	5446	2.09	4.90×10^{-4}	4.05×10^{-4}	8.53×10^{-5}	4.08×10^{-4}
Gaussian curve	5561	2.38	5.64×10^{-4}	4.00×10^{-4}	1.64×10^{-4}	1.13×10^{-3}
Right-angled falling triangle	6030	3.81	5.30×10^{-4}	4.04×10^{-4}	1.25×10^{-4}	6.30×10^{-4}
Right-angled rising triangle	6095	4.09	4.58×10^{-4}	4.10×10^{-4}	7.68×10^{-5}	2.46×10^{-6}
Titanium						
Rectangle	5620	2.02	4.03×10^{-4}	3.97×10^{-4}	6.69×10^{-6}	2.07×10^{-4}
Gaussian curve	5694	2.25	4.21×10^{-4}	3.98×10^{-4}	2.25×10^{-5}	6.34×10^{-4}
Right-angled falling triangle	6082	3.88	4.12×10^{-4}	3.99×10^{-4}	1.33×10^{-5}	4.04×10^{-4}
Right-angled rising triangle	6099	3.94	4.01×10^{-4}	3.92×10^{-4}	8.84×10^{-6}	1.95×10^{-4}

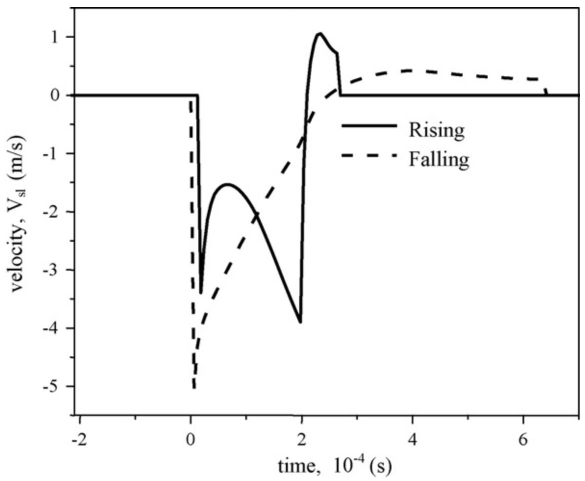

Fig. 5. Evolution of the melting front velocity $\upsilon_{sl}(t)$ for copper: rising (full line) and falling (dashed lime) triangular pulses.

in Fig. 3, appears earlier than in the case of the rectangular pulse. The evaporation front appears much later. Two-humped shape of the dependences $\upsilon_{sl}(t), H_l(t)$ stands for the interaction of the two fronts, Fig. 3. The maximum values of the thickness and the life-time of the liquid phase are the highest among the considered pulses (see Table 1).

3.2. *Influence of the thermophysical properties of the material*

The data in Table 1 present some common regularities for both metals. Thus, the maximum surface temperatures for both metals as function of the laser pulse profile proceed in the following order: rectangle, Gaussian shape, right-angled falling triangle, right-angled rising triangle. The depths of the melt are settled differently: the greatest values are obtained for the Gaussian and the right-angled triangular falling pulses, the smallest ones are for the rectangular and the right-angled triangular rising pulses. For the given pulse duration the maximum thickness of the evaporated layer depends insignificantly on the pulse shape.

In order to assess the influence of the thermophysical parameters of the material over a large range of pulse durations, calculations were carried out for both materials for the case of the rectangular pulse with the intensity $G_{sur} = 10^7$ W cm^{-2} and the duration $\tau_l = 5 \times 10^{-8}$ to 10^{-3} s. Dependencies for the maximum values of the surface temperature $T_{sur,max}(t)$, the evaporation front velocity $\upsilon_{lv,max}(t)$ and the evaporated layer thickness $H_{v,max}(t)$ for copper and titanium are presented in Fig. 6. It may be seen that with the decrease of the pulse duration and, accordingly, with the increase in nonstationarity the surface temperature becomes more dependent of the quantity of the inward heat flux, i.e. of the thermal conductivity coefficient $\lambda(T)$. The ratio between the coefficients of the thermal conductivity of copper and titanium reaches the value $\lambda_{Cu}/\lambda_{Ti} \sim 10$. Consequently, the surface of a titanium target can be heated faster and to higher temperatures, Fig. 6a. Accordingly, for the short pulses

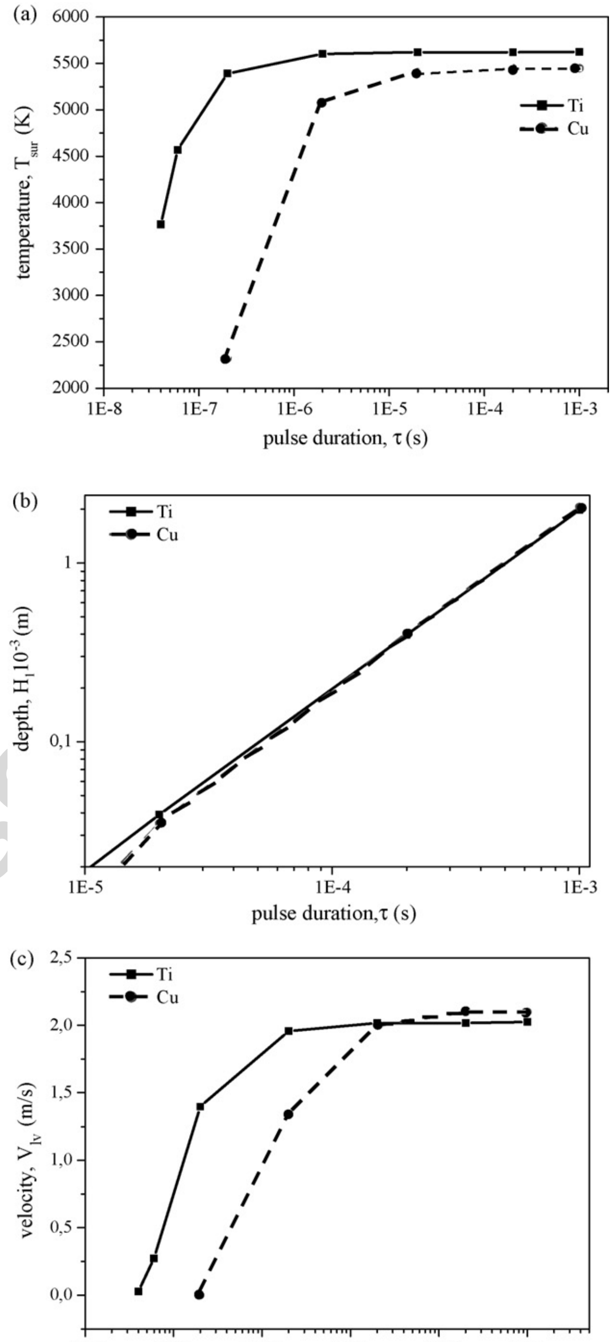

Fig. 6. Surface temperature $T_{sur}(\tau_l)$ (a), evaporated layer thickness $H_v(\tau_l)$ (b) and evaporation front velocity $\upsilon_{lv}(\tau_l)$ (c) vs. pulse duration: titanium (full line), copper (dashed line).

($t \leq 10^{-6}$ s) the material removal from a titanium surface is much higher than from a copper one.

The situation becomes different with the increase of the pulse duration. The thermal conductivity now plays a limited role, although the value $\lambda(T)$ defines the moment when the system reaches stationarity. When the system is settled in steady state, the evaporation front velocity is given by the relationship (2) and depends only on the values of L_v and ρ. In spite of the fact that titanium exhibits the higher value of the steady-state surface temperature, the evaporation rate is smaller owing to the higher heat of vaporization ($L_{v,Ti}/L_{v,Cu} = 2{,}8$) compared to that of copper, Fig. 6b. Consequently, for the long pulses the amount of the evaporated copper is greater in comparison to titanium.

4. Conclusion

Pulsed laser action is characterized by the transient character of the initiated heat phenomena as for example evaporation, melting/solidification, heating/cooling.

It was shown that thermal phenomena initiated by short energy pulses ($\tau_1 \leq 10^{-6}$ s) lead to ablation of a greater quantity of material in the case of metals with low heat conductivity (for example, titanium). The quantity of material evaporated by long duration pulses ($\tau_1 \approx 10^{-4}$ to 10^{-3} s) close to stationary regime depends on the value of specific heat of vaporization and does not depend on heat conductivity of the material. That is why under quasi-stationary conditions the amount of evaporated copper is greater compared to titanium (assuming equality of the quantities of absorbed laser energy).

Variation of the laser pulse shape allows to modify the energy balance between melting/solidification and evaporation processes as well as conductive heat losses that can be used for optimization of different laser applications. Thus, when the depth of penetration is of prime importance, it is better to use pulses with the Gaussian and the right-angled triangular falling temporal profiles. When the presence of the liquid phase is undesirable, the choice of the rectangular and the rising triangular pulses is more appropriate.

Acknowledgments

This study was supported by RFBR grants No. 06-07-87191-a and No. 07-07-00045-a.

References

[1] N. Rykalin, A. Uglov, I. Zuev, A. Kokora, Laser and Electron Material Processing. Handbook, Mir Publishers, Moscow, 1988.
[2] J. Mazumder, Opt. Eng. 30 (8) (1991) 1208–1219.
[3] V.I. Mazhukin, A.A. Samarskii, Surv. Math. Ind. 4 (1994) 85–149.
[4] P.S. Mohanty, A. Kar, J. Mazumder, J. Laser Appl. 8 (1996) 291–297.
[5] A.A. Uglov, I.U. Smurov, A.M. Lashin, A.G. Guskov, Modeling of the Thermophysical Processes in Pulsed Laser Irradiation of Metals, Nauka, Moscow, 1991.
[6] V.I. Mazhukin, V.V. Nossov, U. Semmler, in: Proceedings of the IY Minsk Int. Heat and Mass Transfer Forum, vol. 5, Minsk, (2000), pp. 481–486.
[7] V.I. Mazhukin, I. Smurov, C. Dupuy, D. Jeandel, J. Numer. Heat Transfer Part A 26 (1994) 587–600.
[8] V.I. Mazhukin, M.M. Demin, A.V. Shapranov, I. Smurov, Numer. Heat Transfer Part B: Fundam. 44 (4) (2003) 387–415.
[9] B. Cheynet, J.-D. Dubois, M. Milesi, Données, thermodynamiques des éléments chimiques. Techniques de l'Ingenier, traité Materiaux metalliques, 1993, pp. M64-1–M64-22. Printed in France by Imprimerie Strasbourgeoise.
[10] I.S. Grigoriev, E.Z. Meylikhov, in: I.S. Grigotiev, E.Z. Melikhova (Eds.), Physical Values. Reference Book. M. Energoatomizdat, 1991.
[11] A.A. Samokhin, Effect of laser radiation on absorbing condensed matter, in: A.M. Prokhorov (Ed.), Proceedings of the Institute of General Physics Academy of Sciences of the USSR, vol. 13, Nova Science Publishers, Commack, New York, 1990.